

Compounds with Intermediate Spin. 4.* The Crystal Structure of Tris(*N,N*-dibenzylidithiocarbamato)iron(III) at 150 and 295 K. The Correlation between Temperature-dependent Magnetic Behaviour and Structural Parameters

J. ALBERTSSON, I. ELDING and Å. OSKARSSON

Inorganic Chemistry 1 and 2 and Physical Chemistry 1, Chemical Center, University of Lund,
P.O.B. 740, S-220 07 Lund 7, Sweden

$\text{Fe}[\text{S}_2\text{CN}(\text{CH}_2\text{C}_6\text{H}_5)_2]_3$ has a temperature-dependent magnetic moment. Its crystal structure has been determined with Patterson and Fourier methods from X-ray intensities collected with a four-circle single-crystal diffractometer at 150 K ($\mu_{\text{eff}} = 2.47$) and 295 K ($\mu_{\text{eff}} = 3.45$). At both temperatures the crystals are monoclinic with space group $P2_1$, $Z=4$; $a = 11.888(9)$, $b = 29.573(22)$, $c = 12.313(7)$ Å, $\beta = 98.33(6)^\circ$ at 150 K; $a = 11.884(3)$, $b = 29.906(8)$, $c = 12.472(3)$ Å, $\beta = 97.84(2)^\circ$ at 295 K. The least-squares refinements converged to $R = 0.063$ at both temperatures. The structure comprises two independent mononuclear tris(*N,N*-dibenzylidithiocarbamato)iron(III) complexes of symmetry $\sim D_3$ kept together by van der Waals forces. Their geometries are compared with the geometries of four other iron(III) dithiocarbamate complexes studied at low and room temperature. The main structural difference between low and high-spin complexes is the Fe–S bond length. A change in μ_{eff} (*i.e.* a change in T) results in a change in Fe–S and a small change in the geometry of the FeS_6 core but has no discernible effect on the ligand, except for a small change of the ligand bite.

It is well known that most complexes formed between iron(III) and substituted dithiocarbamato ligands exhibit strongly temperature dependent magnetic moments.^{1–3} As described in the first paper of the present series⁵ essentially two models of the temperature dependent spin-state have been

proposed: (i) a thermal equilibrium between the low-spin 2T_2 and high-spin 6A_1 states of iron(III) (assuming O_h symmetry of the FeS_6 core)^{2,3} and (ii) a spin-mixed state caused by spin-orbit coupling between low-lying sextet, quartet and doublet states in the trigonally distorted FeS_6 core.^{5–7} EPR⁸ and IR⁹ experiments favour model (i) with a frequency for the cross-over between the electronic levels in the range 10^7 – 10^{10} Hz.^{5,10} So far, X-ray diffraction experiments have not been able to distinguish between the two models since thermal smearing prevents the resolution of the high and low-spin complexes of model (i) except at very low temperatures.¹¹

In the iron(III) dithiocarbamates, $\text{Fe}(\text{S}_2\text{CNR}_2)_3$, the partially filled d orbitals of iron may interact with empty ligand π orbitals arising from the d orbitals of sulfur.^{10,12} This back-donation, the inductive strength of the substituent R , and steric interference caused by R should result in a variable partial double-bond character of the S–C and C–N bonds (Fig. 1). Cukauskas^{13,14} has shown that tris(1-pyrrolidinylcarbodithiato-S,S')iron(III) is antiferromagnetic with a Néel temperature as high as about 2 K in spite of the very long Fe–Fe distances (8.7 Å). The ligands are in van der Waals contact in the solid complex and their electronic properties, or rather the electronic properties of the group in Fig. 1 thus appear to be essential for the magnetic interaction of the iron(III) dithiocarbamate complexes.

The present series of investigation aims at correlating the temperature dependent magnetic be-

* For part 3 in this series, see Ref. 15.

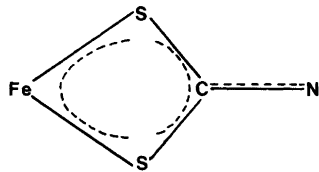


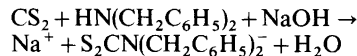
Fig. 1. The bonding in FeS_2CN .

haviour of some solid iron(III) dithiocarbamates with the geometrical features of the complexes: (i) the symmetry of the FeS_6 core, (ii) bond distances and angles in the FeS_6 core and S_2CNC_2 group, (iii) the conformation of the ligand molecule, and (iv) the crystal packing of the iron(III) complexes.

Here we report the crystal structure of tris(*N,N*-dibenzylidithiocarbamato)iron(III) at 150 K ($\mu_{\text{eff}} = 2.47$) and 295 K ($\mu_{\text{eff}} = 3.45$) and compare the geometrical parameters obtained with those of the four other iron(III) dithiocarbamates whose crystal structures have been determined both at low and room temperature.^{4,11,15,16}

EXPERIMENTAL

The sodium salt of the *N,N*-dibenzylidithiocarbamato ligand was prepared as an 0.1 mol l⁻¹ ethanol solution by mixing equal amounts of carbon disulfide, dibenzylamine and sodium hydroxide



The iron complex was precipitated by adding an ethanol solution of anhydrous FeCl_3 . Black, prismatic single crystals were grown from a chloroform solution of the precipitate by slowly adding water-free ethanol. All preparations were made in nitrogen atmosphere.

Magnetic susceptibility measurements were made by Nygren¹⁷ with the Faraday method using an automatic balance described elsewhere.¹⁸ The result for $\text{Fe}[\text{S}_2\text{CN}(\text{CH}_2\text{C}_6\text{H}_5)_2]_3$ and some other iron(III) dithiocarbamates is shown in Fig. 2 where the effective magnetic moment, μ_{eff} , is plotted vs. the temperature.

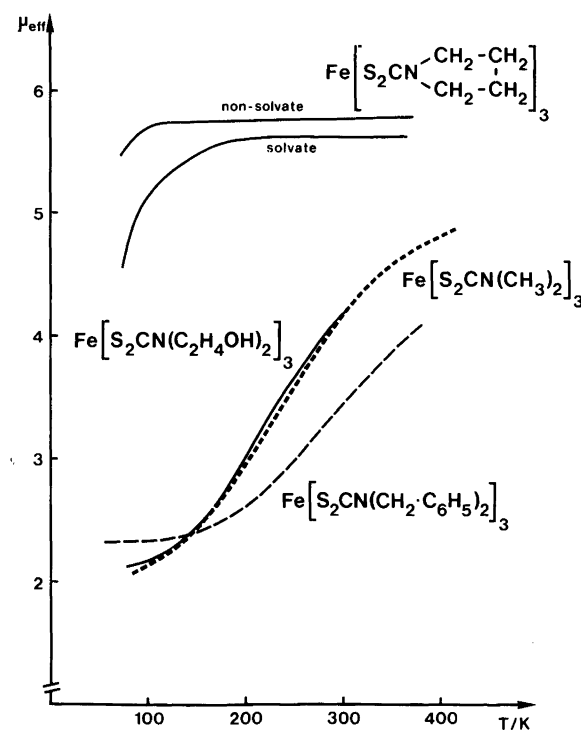


Fig. 2. The effective magnetic moment, μ_{eff} , of some iron(III) dithiocarbamates as a function of temperature. The measurements were made with the Faraday method.^{17,18}

Table 1. The unit cell dimensions of $\text{Fe}[\text{S}_2\text{CN}(\text{CH}_2\text{C}_6\text{H}_5)_2]_3$ in the interval 150–295 K.

T/K	a/Å	b/Å	c/Å	$\beta/^\circ$	V/Å ³
295	11.884(3)	29.906(8)	12.472(3)	97.84(2)	4391
250	11.889(4)	29.777(12)	12.419(4)	98.05(3)	4353
225	11.889(3)	29.660(10)	12.392(3)	98.14(3)	4326
200	11.893(5)	29.632(14)	12.356(4)	98.22(4)	4310
175	11.878(6)	29.556(14)	12.330(5)	98.28(4)	4284
150	11.888(9)	29.573(22)	12.313(7)	98.33(6)	4283

Preliminary Weissenberg photographs revealed the Laue class $2/m$ and systematic absences $0k0$, $k=2n+1$, which are consistent with the space groups $P2_1$ and $P2_1/m$. Since the peaks of the subsequent vector map were compatible with the polar space group $P2_1$ and $Z=4$, but not with $P2_1/m$, $P2_1$ was chosen (the peaks were concentrated in the plane $x \frac{1}{2} z$ only¹⁹). The space group does not change on cooling. The rest of the X-ray investigation was carried out using an automatic four-circle diffractometer of type CAD4 equipped with a low-temperature device described before.²⁰ Table 1 gives the unit-cell dimensions at six temperatures in the interval 150–295 K. They were

determined from about 50 θ -values measured at each temperature as described in Ref. 20. MoK α -radiation was used ($\lambda\alpha_1=0.709300$ Å).

The crystal data, experimental parameters pertinent to the collection and reduction of the intensity data sets, and some information about the least-squares refinements are given in Table 2. During each intensity data collection three standard reflexions were checked at regular intervals. No systematic variation in their intensities was observed. The values of I and $\sigma_c(I)$ were corrected for Lorentz, polarization and absorption effects [$\sigma_c(I)$ is based on counting statistics]. Since graphite-monochromated radiation was used for the data set at

Table 2. Crystal data, collection and reduction of the intensities and the least-squares refinements. Unit cell dimensions are given in Table 1.

Compound	Tris(<i>N,N</i> -dibenzylidithiocarbamato)iron(III)	
Formula	$\text{C}_{45}\text{H}_{42}\text{FeN}_3\text{S}_6$	
M_r	873.05	
Space group	$P2_1$	
Z	4	
T(K)	150	295
ρ_{calc} (g cm ⁻³)	1.35	1.32
Crystal size (mm)	0.34 × 0.17 × 0.09	0.16 × 0.22 × 0.16
Radiation (MoK α)	Zr-filtered	Graphite-monochromated
Take-off angle (°)	3	3
$\Delta\omega$ (°) ($\omega - 2\theta$ scan)	1.0 + 1.0 tan θ	0.7 + 1.0 tan θ
θ -interval (°)	3–20	3–23
Min. number of counts in a scan	3000	3000
Max. recording time (s)	180	180
μ (cm ⁻¹)	6.75	6.60
Range of the transmission factor	0.835–0.912	0.872–0.920
No. of measured reflexions	4278	6526
No. of independent reflexions, m , used in the final refinement [$I > 2\sigma_c(I)$]	2512	3868
No. of parameters refined, n	512	574
$R = \sum \Delta F /\sum F_o ^a$	0.063	0.063
$R_w = [\sum w(\Delta F)^2/\sum w F_o ^2]^{1/2}$	0.068	0.073
$S = [\sum w(\Delta F)^2/(m-n)]^{1/2}$	1.70	1.62
C (weighting function)	0.020	0.025

^a $\Delta F = |F_o| - |F_c|$.

Table 3. Positional ($\times 10^4$) and isotropic thermal parameters of the non-hydrogen atoms with e.s.d.'s.

150 K				295 K				
	x	y	z	B/ \AA^2	x	y	z	B/ \AA^2
Fe(1)	-32(3)	0(0)	889(3)		-29(2)	0(0)	876(2)	
Fe(2)	5518(2)	2494(1)	4675(3)		5519(2)	2511(1)	4611(2)	
S(1)	-275(5)	-189(2)	-941(5)		-258(4)	-196(2)	-948(4)	
S(2)	1051(5)	527(2)	84(5)		1069(4)	523(2)	49(4)	
S(3)	1308(5)	-555(3)	1384(5)		1317(4)	-564(2)	1412(4)	
S(4)	623(5)	142(2)	2716(5)		603(4)	142(2)	2703(4)	
S(5)	-1619(5)	-438(2)	1085(5)		-1663(4)	-434(1)	1086(4)	
S(6)	-1521(5)	507(3)	750(5)		-1534(4)	503(1)	751(4)	
S(7)	5750(5)	2703(2)	6483(5)		5741(4)	2717(2)	6409(4)	
S(8)	4497(5)	1958(3)	5492(5)		4466(4)	1986(2)	5451(4)	
S(9)	7077(5)	2019(2)	4902(5)		7078(4)	2031(1)	4824(4)	
S(10)	7025(5)	2953(2)	4342(5)		7058(3)	2954(1)	4279(4)	
S(11)	4110(5)	3007(2)	4106(5)		4107(4)	3024(2)	4031(3)	
S(12)	4957(5)	2311(2)	2860(5)		4940(4)	2323(4)	2808(4)	
N(1)	546(14)	452(6)	-2095(15)	2.2(4)	535(10)	442(4)	-2128(11)	
N(2)	1997(14)	-526(7)	3535(14)	2.3(4)	1973(10)	-510(4)	3556(10)	
N(3)	-3533(14)	66(7)	426(14)	2.5(4)	-3506(11)	74(4)	462(10)	
N(4)	5010(14)	2044(6)	7705(15)	1.9(4)	4995(10)	2064(4)	7610(11)	
N(5)	9000(12)	2503(6)	4834(13)	1.5(4)	8996(9)	2496(4)	4768(10)	
N(6)	3674(14)	2989(6)	1920(15)	2.2(4)	3635(10)	2981(4)	1856(10)	
C(1)	440(17)	278(8)	-1129(18)	.9(5)	507(13)	279(6)	-1158(14)	
C(16)	1375(17)	-374(8)	2684(18)	2.0(5)	1387(13)	-342(6)	2678(13)	
C(31)	-2366(18)	25(8)	739(18)	2.4(5)	-2397(13)	54(5)	758(12)	
C(46)	5041(18)	2210(8)	6683(19)	2.4(6)	5053(12)	2228(5)	6599(13)	
C(61)	7840(16)	2492(8)	4678(16)	1.6(5)	7896(12)	2489(6)	4629(11)	
C(76)	4166(17)	2782(7)	2796(17)	1.3(5)	4145(10)	2804(3)	2772(10)	
C(2)	-23(18)	230(8)	-3119(19)	2.5(6)	-36(12)	248(5)	-3092(13)	4.5(3)
C(3)	-1106(17)	486(8)	-3593(18)	2.9(5)	-1130(13)	481(5)	-3536(13)	5.0(3)
C(4)	-1499(18)	459(8)	-4737(19)	3.1(5)	-1433(16)	481(6)	-4669(16)	7.3(5)
C(5)	-2502(21)	640(9)	-5167(20)	4.5(6)	-2454(17)	661(7)	-5129(16)	8.2(5)
C(6)	-3167(20)	849(9)	-4503(22)	4.5(6)	-3106(16)	872(7)	-4451(17)	7.6(5)
C(7)	-2874(18)	889(8)	-3398(19)	2.9(5)	-2864(16)	888(7)	-3364(18)	7.7(5)
C(8)	-1842(18)	666(8)	-2934(18)	3.0(5)	-1833(17)	656(7)	-2912(17)	7.9(5)
C(9)	1178(18)	874(8)	-2255(19)	2.9(6)	1151(14)	858(6)	-2274(14)	5.5(4)
C(10)	2127(17)	782(8)	-2908(18)	2.8(5)	2150(13)	768(5)	-2904(13)	4.9(4)
C(11)	3032(17)	518(7)	-2407(17)	2.5(5)	3056(15)	501(6)	-2459(15)	6.9(4)
C(12)	3912(17)	380(7)	-3015(18)	3.0(5)	3911(14)	408(6)	-3140(16)	6.7(4)
C(13)	3865(18)	553(8)	-4071(18)	2.8(5)	3817(15)	587(6)	-4161(16)	6.3(5)
C(14)	3025(21)	807(9)	-4517(21)	4.3(6)	2949(15)	825(6)	-4555(15)	6.7(4)
C(15)	2117(18)	927(8)	-3930(19)	3.1(5)	2114(14)	931(6)	-3934(15)	5.9(4)
C(17)	2712(18)	-917(8)	3493(18)	2.5(6)	2702(12)	-897(5)	3501(12)	4.2(3)
C(18)	3952(16)	-790(7)	3526(16)	1.6(4)	3930(12)	-773(5)	3572(11)	4.1(3)
C(19)	4272(17)	-404(7)	3059(16)	2.6(5)	4261(14)	-376(6)	3118(13)	6.1(4)
C(20)	5406(22)	-318(10)	3082(21)	5.3(7)	5423(16)	-298(7)	3176(16)	8.1(5)
C(21)	6240(19)	-574(8)	3546(18)	3.5(6)	6224(17)	-592(8)	3622(17)	8.1(5)
C(22)	5918(17)	-973(8)	4013(17)	2.1(5)	5900(15)	-968(6)	4052(14)	6.6(4)
C(23)	4776(17)	-1092(7)	3963(17)	2.4(5)	4764(14)	-1068(5)	4014(13)	5.7(4)
C(24)	2027(18)	-362(8)	4664(19)	3.2(6)	1978(13)	-334(6)	4648(13)	6.0(4)
C(25)	1231(17)	-612(8)	5356(17)	2.5(5)	1224(13)	-584(5)	5311(13)	5.3(4)
C(26)	130(19)	-681(8)	4935(19)	3.3(5)	133(15)	-666(6)	4954(15)	6.3(4)
C(27)	-561(20)	-878(9)	5600(21)	4.1(6)	-649(17)	-880(7)	5603(18)	8.1(5)
C(28)	-142(20)	-1038(9)	6616(21)	4.4(6)	-93(16)	-1021(6)	6580(16)	7.1(5)
C(29)	932(22)	-954(9)	7022(20)	4.3(6)	945(18)	-954(7)	6966(16)	8.0(5)
C(30)	1716(20)	-722(8)	6398(20)	3.9(6)	1714(18)	-718(7)	6344(18)	8.7(6)

Table 3. Continued.

C(32)	-4105(19)	499(8)	110(19)	3.0(6)	-4100(13)	491(5)	142(13)	5.3(4)
C(33)	-4662(15)	698(7)	1017(15)	1.3(4)	-4639(11)	690(4)	1012(11)	3.7(3)
C(34)	-5785(16)	568(7)	1116(16)	2.0(5)	-5768(12)	569(5)	1143(12)	5.2(3)
C(35)	-6243(17)	753(8)	2003(17)	2.6(5)	-6229(14)	759(6)	2012(14)	6.0(4)
C(36)	-5649(18)	1046(8)	2726(18)	3.3(5)	-5618(14)	1052(6)	2688(14)	5.8(4)
C(37)	-4521(16)	1155(7)	2605(17)	2.3(5)	-4514(14)	1153(6)	2606(14)	5.5(4)
C(38)	-4029(15)	972(6)	1772(15)	1.1(4)	-4056(11)	964(5)	1768(11)	3.9(3)
C(39)	-4151(16)	-342(8)	173(17)	2.3(5)	-4152(13)	-351(6)	241(13)	5.8(4)
C(40)	-4251(17)	-430(8)	-1078(17)	2.9(5)	-4252(15)	-467(6)	-1015(15)	6.4(4)
C(41)	-3470(16)	-303(7)	-1687(17)	2.5(5)	-3517(14)	-309(6)	-1655(15)	6.2(4)
C(42)	-3558(18)	-412(8)	-2804(18)	3.1(5)	-3618(18)	-423(8)	-2765(18)	8.7(6)
C(43)	-4416(20)	-691(9)	-3239(19)	4.0(6)	-4470(19)	-701(8)	-3121(19)	8.5(6)
C(44)	-5174(19)	-872(8)	-2614(21)	4.0(6)	-5230(15)	-852(6)	-2566(16)	6.8(4)
C(45)	-5103(18)	-767(8)	-1549(19)	3.1(5)	-5150(17)	-755(7)	-1502(18)	7.9(5)
C(47)	5625(18)	2280(8)	8701(19)	2.7(6)	5566(12)	2283(5)	8608(12)	4.7(3)
C(48)	6686(16)	2039(7)	9172(17)	2.2(5)	6649(11)	2055(4)	9061(11)	4.2(3)
C(49)	6931(18)	1998(8)	10314(18)	3.0(5)	6908(13)	1985(6)	10158(14)	6.2(4)
C(50)	7959(20)	1804(8)	10738(19)	3.9(6)	7948(16)	1777(6)	10570(16)	7.8(5)
C(51)	8727(19)	1660(8)	10083(20)	3.5(6)	8642(17)	1664(7)	9874(18)	8.5(5)
C(52)	8476(22)	1736(9)	8966(23)	5.3(7)	8476(16)	1728(6)	8843(17)	7.8(5)
C(53)	7463(19)	1903(8)	8502(18)	3.1(5)	7460(14)	1907(6)	8388(14)	6.6(4)
C(54)	4353(18)	1629(8)	7861(19)	2.6(5)	4337(12)	1649(5)	7794(12)	4.5(3)
C(55)	3316(17)	1782(7)	8430(17)	2.3(5)	3341(12)	1775(5)	8363(12)	4.4(3)
C(56)	3199(20)	1651(8)	9504(21)	4.1(6)	3275(13)	1631(5)	9408(13)	5.9(4)
C(57)	2276(19)	1787(8)	10012(19)	3.3(5)	2323(15)	1773(6)	9909(15)	6.9(4)
C(58)	1525(19)	2064(8)	9402(20)	3.8(6)	1541(14)	2043(6)	9386(14)	6.4(4)
C(59)	1590(21)	2211(9)	8355(23)	5.1(7)	1579(14)	2213(6)	8367(15)	7.1(4)
C(60)	2482(18)	2075(8)	7861(18)	3.1(5)	2534(14)	2048(6)	7875(14)	6.3(4)
C(62)	9687(16)	2896(7)	4640(16)	1.5(5)	9687(12)	2898(5)	4592(12)	4.4(3)
C(63)	10256(18)	3091(8)	5676(17)	2.9(5)	10253(13)	3079(5)	5615(12)	5.3(3)
C(64)	9648(20)	3219(8)	6504(20)	3.7(6)	9666(17)	3186(7)	6415(19)	9.2(5)
C(65)	10211(24)	3425(10)	7444(23)	5.9(7)	10249(24)	3413(10)	7414(23)	13.2(8)
C(66)	11364(23)	3451(9)	7627(22)	5.2(7)	11384(21)	3451(8)	7468(19)	10.0(6)
C(67)	11986(19)	3289(8)	6870(20)	3.8(6)	11948(18)	3280(7)	6772(20)	9.6(6)
C(68)	11429(20)	3118(8)	5883(20)	3.8(6)	11428(16)	3108(6)	5818(16)	7.6(5)
C(69)	9658(17)	2093(8)	5283(17)	2.2(5)	9664(12)	2103(5)	5195(12)	4.7(4)
C(70)	10207(17)	1853(7)	4389(17)	2.3(5)	10162(11)	1856(4)	4280(11)	4.1(3)
C(71)	11286(16)	1926(7)	4179(16)	2.2(5)	11302(12)	1926(5)	4131(12)	5.3(3)
C(72)	11769(19)	1715(8)	3347(19)	3.3(5)	11737(14)	1700(6)	3260(14)	6.5(4)
C(73)	11081(19)	1416(8)	2739(19)	3.4(6)	11101(15)	1421(6)	2636(15)	6.8(4)
C(74)	10041(20)	1295(9)	2924(20)	4.0(6)	10080(16)	1323(7)	2802(16)	7.8(5)
C(75)	9602(20)	1515(9)	3739(21)	4.2(6)	9559(13)	1530(5)	3652(14)	6.2(4)
C(77)	3844(18)	2817(8)	818(19)	3.0(6)	3817(12)	2802(5)	792(12)	4.6(3)
C(78)	4685(16)	3106(7)	350(17)	2.1(5)	4619(11)	3092(5)	283(12)	4.6(3)
C(79)	4351(18)	3325(8)	-655(18)	2.7(5)	4239(13)	3315(5)	-734(13)	6.0(4)
C(80)	5195(20)	3570(8)	-1118(18)	3.0(6)	5028(15)	3554(6)	-1216(14)	6.8(4)
C(81)	6230(20)	3600(8)	-609(20)	3.5(6)	6092(15)	3601(6)	-736(15)	6.7(4)
C(82)	6577(19)	3374(8)	357(20)	3.8(6)	6509(16)	3399(7)	225(17)	8.5(5)
C(83)	5776(17)	3123(7)	860(17)	2.4(5)	5732(13)	3130(5)	744(12)	5.3(3)
C(84)	2842(18)	3390(8)	1857(18)	2.8(6)	2853(12)	3363(5)	1842(12)	4.7(4)
C(85)	1632(17)	3202(8)	1532(17)	2.4(5)	1651(11)	3227(4)	1505(11)	3.7(3)
C(86)	1261(17)	2825(7)	1979(17)	2.1(5)	1225(12)	2839(5)	1913(12)	5.0(3)
C(87)	159(17)	2669(8)	1678(17)	2.5(5)	102(14)	2688(6)	1629(14)	6.2(4)
C(88)	-551(19)	2920(9)	892(20)	4.1(6)	-552(16)	2947(7)	865(16)	7.9(5)
C(89)	-176(19)	3287(8)	429(19)	3.3(6)	-156(15)	3327(6)	488(15)	7.2(4)
C(90)	925(17)	3465(8)	780(18)	2.4(5)	946(12)	3465(5)	800(12)	5.1(3)

295 K, the approximate expression $p = (\cos^2 2\theta_M + \cos^2 \theta)/(1 + \cos^2 2\theta_M)$ was used when these intensities were corrected for polarization ($\theta_M = 6.08^\circ$ for MoK α -radiation).

The positions of two independent iron atoms were deduced from the vector map. Subsequent difference syntheses revealed all the 110 non-

hydrogen atoms in the asymmetric unit. Anisotropic thermal parameters were assigned to Fe and S at 150 K and to Fe and the atoms in the S₂CN groups at 295 K. More than 500 parameters are then required to describe the structure of the non-hydrogen atoms. Therefore, the parameters were partitioned in three blocks treated individually by

Table 4. Anisotropic thermal parameters with e.s.d.'s. The form of the temperature factor is $\exp(-\beta_{11}h^2 - 2\beta_{12}hk\dots)$.

	β_{11}	β_{22}	β_{33}	β_{12}	β_{13}	β_{23}
150 K ($\times 10^5$)						
Fe1	354(32)	80(6)	369(32)	27(12)	28(27)	6(12)
Fe2	406(27)	65(5)	419(27)	-1(10)	113(22)	12(10)
S1	425(60)	63(11)	421(58)	3(19)	143(52)	-28(21)
S2	432(59)	94(12)	347(58)	-12(22)	-1(49)	-1(22)
S3	411(61)	90(11)	450(62)	31(21)	75(53)	-45(22)
S4	593(64)	82(12)	369(58)	45(21)	86(51)	26(21)
S5	585(64)	66(11)	526(61)	24(21)	131(56)	-2(22)
S6	387(59)	81(11)	506(63)	20(20)	-3(49)	-33(22)
S7	614(70)	57(10)	419(59)	-28(21)	-15(55)	32(22)
S8	504(63)	88(11)	384(62)	-37(23)	53(52)	-6(22)
S9	407(59)	31(9)	599(63)	6(19)	132(50)	36(20)
S10	458(60)	47(10)	475(59)	28(19)	49(53)	34(21)
S11	523(63)	89(11)	309(57)	64(21)	123(50)	18(21)
S12	372(60)	63(11)	467(62)	77(19)	116(52)	-24(21)
295 K ($\times 10^4$)						
Fe1	87(2)	12(0)	76(2)	3(1)	14(2)	-1(1)
Fe2	76(2)	11(0)	74(2)	-3(1)	20(2)	3(1)
S1	105(4)	15(1)	79(4)	-8(1)	18(4)	-5(1)
S2	97(4)	16(1)	78(4)	-8(1)	8(3)	-6(1)
S3	107(4)	15(1)	77(4)	9(1)	18(4)	-5(1)
S4	115(5)	14(1)	98(5)	13(1)	23(4)	-5(1)
S5	104(4)	10(1)	93(4)	5(1)	27(4)	3(1)
S6	89(4)	11(1)	100(4)	0(1)	-4(3)	2(1)
S7	115(5)	13(1)	75(4)	-12(1)	12(4)	3(1)
S8	94(4)	14(1)	69(4)	-9(1)	4(3)	0(1)
S9	89(4)	10(1)	107(4)	-5(1)	16(4)	5(1)
S10	76(4)	10(1)	96(4)	0(1)	9(3)	3(1)
S11	104(4)	13(1)	67(4)	4(1)	25(3)	-4(1)
S12	97(4)	11(1)	79(4)	3(1)	23(3)	-2(1)
N1	91(12)	12(2)	61(11)	-11(4)	19(10)	0(4)
N2	82(12)	12(2)	71(11)	2(4)	19(10)	-8(4)
N3	97(13)	8(2)	81(12)	-4(4)	0(10)	-3(4)
N4	84(12)	12(2)	81(12)	5(4)	-2(10)	-6(4)
N5	63(11)	13(2)	75(10)	1(4)	-2(9)	3(4)
N6	67(11)	13(2)	70(11)	11(4)	14(9)	1(4)
C1	55(14)	21(3)	69(16)	-4(5)	21(12)	-5(6)
C16	79(16)	20(3)	56(14)	-3(6)	6(12)	-7(6)
C31	78(15)	11(2)	66(13)	-12(5)	-11(12)	-2(5)
C46	73(15)	15(3)	62(14)	5(5)	-4(12)	6(5)
C61	50(13)	21(3)	52(13)	10(5)	4(11)	-6(5)
C76	82(11)	1(1)	84(12)	-1(3)	46(10)	-1(3)

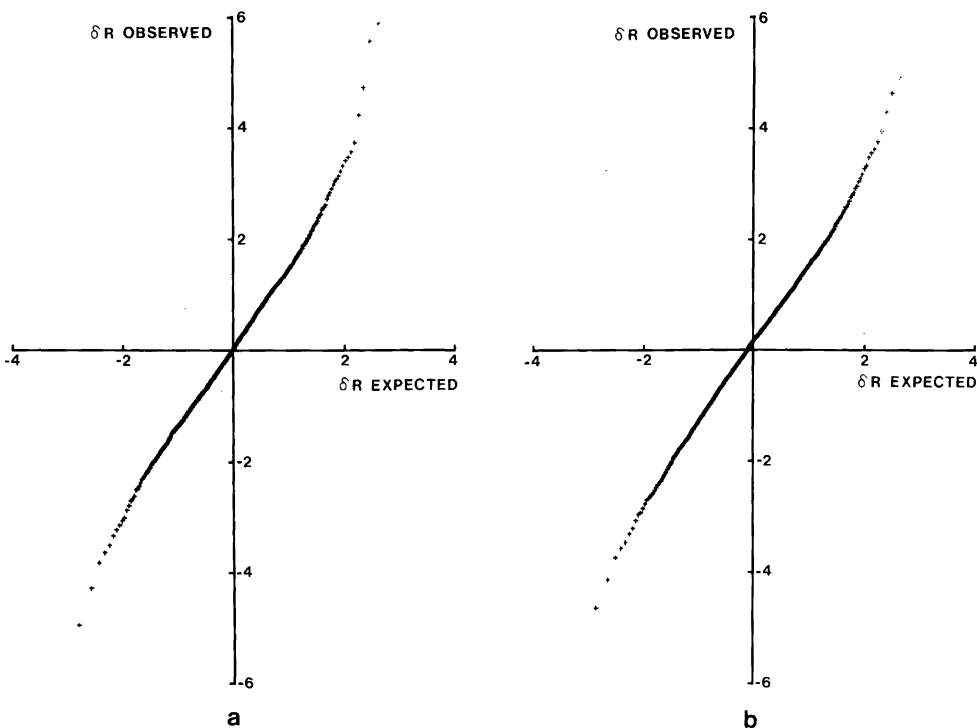


Fig. 3. δR -plot comparison of data and models for $\text{Fe}[\text{S}_2\text{CN}(\text{CH}_2\text{C}_6\text{H}_5)_2]_3$: (a) 150 K, slope: 1.52, intercept: 0.07; (b) 295 K, slope: 1.48, intercept: 0.12.

full-matrix least-squares refinement minimizing $\sum w(\Delta F)^2$ with weights $w = [(\sigma_c^2/4)|F_o|^2 + C^2|F_o|^2]^{-1}$ (Table 2). C was adjusted so that constant values of $\langle w(\Delta F)^2 \rangle$ were obtained in different $|F_o|$ and $\sin \theta$ intervals. Before the last cycles of refinement the positions of 84 hydrogen atoms (all belonging to phenyl and CH_2 groups) were calculated from geometrical considerations and included in the structure factor calculations with fixed coordinates ($B = 5.0 \text{ \AA}^2$ at 295 K and 3.0 \AA^2 at 150 K). This improved a number of phenyl C—C distances.

The atomic scattering factors were taken from *International Tables for X-Ray Crystallography*²¹ with the factors for iron and sulfur atoms corrected for anomalous dispersion. Table 3 gives the positional parameters of the non-hydrogen atoms and Table 4 the anisotropic thermal parameters.* For each of the two crystals investigated both absolute configurations were tested against the data. A

slightly better fit is obtained with the models of Table 3 than with the mirror related ones (*i.e.*, the data may be taken to indicate the same absolute configuration for the two specimens). Data and final models are compared by probability-plotting in Fig. 3 where ordered values of $\delta R_i = \Delta F_i / \sigma(|F_{oi}|)$ ($\sigma(|F_{oi}|) = w^{-1/2}$) are plotted *vs.* those expected for ordered normal deviates.²² Both plots are rather straight lines with small intercepts so the systematic errors of measurements appear to be small, but the slopes (and the related S -values of Table 2) indicate that $\sigma(|F_o|)$ is on average underestimated, probably by a factor of about 1.5 at both temperatures.

RESULTS

The structure of tris(*N,N*-dibenzylthiocarbamato)iron(III) comprises two independent mono-nuclear complexes. Fig. 4 shows stereoscopic pairs of drawings of them. There are only van der Waals forces between the complexes. Fig. 5 shows the resulting packing arrangement. Fe(1)—Fe(2) is the

* The calculated positions of the hydrogen atoms and lists of $|F_o|$ and $|F_c|$ for the reflexions used in the refinements can be obtained from one of the authors (J.A.) on request.

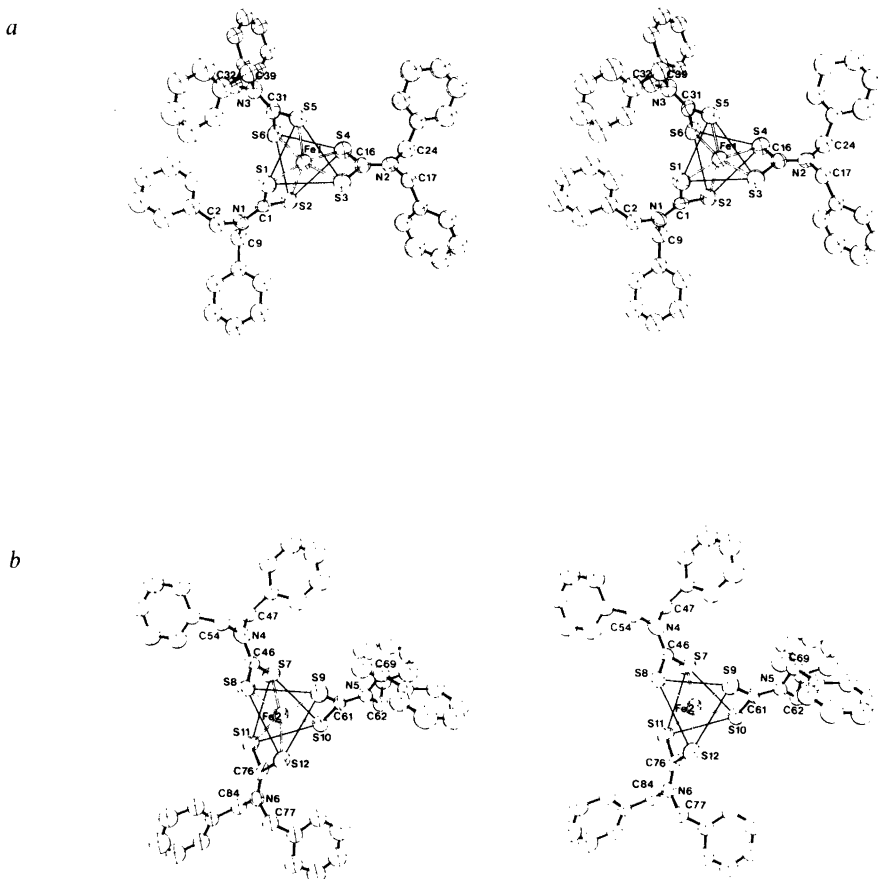


Fig. 4. Stereoscopic pairs of drawings of the two independent complexes in solid $\text{Fe}[\text{S}_2\text{CN}(\text{CH}_2\text{C}_6\text{H}_5)_2]_3$. The thermal ellipsoids (at 295 K) are scaled to include 50 % probability. The atomic numbering is given for (a) Complex 1, (b) Complex 2.

shortest distance between two iron atoms; it is 10.54 Å at 150 K and 10.61 Å at 295 K.

The Fe(1) and Fe(2) complexes have opposite chiralities. Apart from this, the observed geometries are almost the same. Table 5 gives selected interatomic distances in the coordination polyhedra. They are twisted trigonal prisms of symmetry $\sim D_3$. The torsion (twist) angles are 40–43°. The mean observed Fe–S distances decrease from 2.349(8) Å at 295 K to 2.314 Å at 150 K [Fe(1)–S] and from 2.327(6) to 2.306(6) Å [Fe(2)–S]. This is accompanied by a decrease in the unit-cell volume from 4391 to 4283 Å³ (Table 1) which thus may reflect the decreasing size of the FeS_6 cores when μ_{eff} decreases (Fig. 1) but also a

more efficient crystal packing at 150 than at 295 K caused by the decrease in intermolecular thermal motion.

Selected bond distances and angles in the six ligand molecules are given in Table 6. There are 57 bond distances between the non-hydrogen ligand atoms in each complex. These distances, d_i , are compared by probability-plotting in Figs. 5 *a* and *b*. The method is discussed elsewhere.²³ Ordered values of $\delta d_i = |\Delta d_i|/\sigma(\Delta d)$ are plotted *vs.* the expectation values for a half-normal distribution with zero mean and unit variances. The three ligands in the Fe(1) complex can be compared with the three ligands in the Fe(2) complex in three different ways after reversion of the chirality. We have chosen the

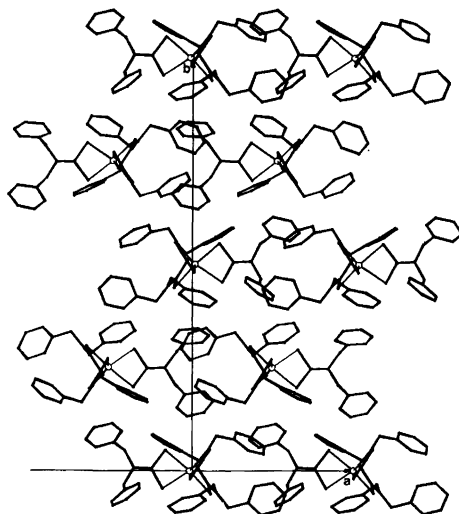


Fig. 5. The crystal packing of $\text{Fe}[\text{S}_2\text{CN}(\text{CH}_2\text{C}_6\text{H}_5)_2]_3$. The space group is $P2_1$.

one with the best molecular fit of the FeS_6 -cores. The bond distances of ligands 1 and 4, 2 and 6, and 3 and 5 are compared. The curves in Fig. 6 *a* and *b* are almost straight lines with zero intercepts. The slopes, 1.18 at 150 K and 1.40 at 295 K, indicate that the interatomic distances have somewhat under-

estimated standard deviations, as could be expected from the δR -plots (Fig. 3) and the *S*-values (Table 2).

Fig. 6 *c* is a comparison of all the 114 ligand bond lengths at 150 and 295 K. The bond lengths are not corrected for effects caused by thermal motion. That the line in Fig. 6 *c* has the intercept -0.04 and is as straight as those in Figs. 6 *a* and *b* implies that the errors possibly introduced by not correcting for thermal motion are negligible. All intramolecular distances less than 2.90 Å are included in the comparison of the six ligand molecules at 150 and 295 K shown in Fig. 6 *d*. We conclude that also the bond angles are the same at both temperatures. The decrease in $\text{Fe}-\text{S}$ with temperature is not large enough in this compound to cause a significant decrease in the angle $\text{S}-\text{C}-\text{S}$ as it is, e.g., in tris(*N,N*-dimethylthiocarbamato)-iron(III) and tris[*N,N*-di(2-hydroxyethyl)dithiocarbamato]iron(III).^{4,15} The decrease in the mean observed $\text{S}-\text{S}$ distance (the ligand bite) is from 2.844(3) Å at 295 K to 2.834(3) Å at 150 K (Table 5).

Table 7 gives deviations from the least-squares planes through the six S_2CN groups. Neither $\text{Fe}(1)$ nor $\text{Fe}(2)$ is located in the intersection of the three ligand planes of the complexes. Eleven of the twelve CH_2 carbon atoms are less than 0.17 Å from their ligand planes, while C(39) deviates 0.3 Å. On the whole, the six $\begin{array}{c} \text{S} \\ \diagup \\ \text{C} \\ \diagdown \\ \text{N} \\ \diagup \\ \text{C} \\ \diagdown \\ \text{C} \end{array}$ groups are planar but

Table 5. Selected interatomic distances (Å) in the FeS_6 polyhedra.

Complex 1	150 K	295 K	Complex 2	150 K	295 K
$\text{Fe}(1)-\text{S}(1)$	2.299(7)	2.329(5)	$\text{Fe}(2)-\text{S}(7)$	2.288(7)	2.306(5)
$\text{Fe}(1)-\text{S}(2)$	2.332(7)	2.362(5)	$\text{Fe}(2)-\text{S}(8)$	2.315(8)	2.342(5)
$\text{Fe}(1)-\text{S}(3)$	2.307(7)	2.357(5)	$\text{Fe}(2)-\text{S}(9)$	2.310(7)	2.328(5)
$\text{Fe}(1)-\text{S}(4)$	2.309(7)	2.339(5)	$\text{Fe}(2)-\text{S}(10)$	2.330(7)	2.341(5)
$\text{Fe}(1)-\text{S}(5)$	2.330(7)	2.380(5)	$\text{Fe}(2)-\text{S}(11)$	2.291(7)	2.316(5)
$\text{Fe}(1)-\text{S}(6)$	2.308(7)	2.327(5)	$\text{Fe}(2)-\text{S}(12)$	2.303(7)	2.329(5)
$\text{S}(1)-\text{S}(2)$	2.827(9)	2.850(7)	$\text{S}(7)-\text{S}(8)$	2.834(10)	2.830(6)
$\text{S}(3)-\text{S}(4)$	2.826(10)	2.854(7)	$\text{S}(9)-\text{S}(10)$	2.844(10)	2.842(6)
$\text{S}(5)-\text{S}(6)$	2.832(10)	2.842(6)	$\text{S}(11)-\text{S}(12)$	2.839(9)	2.847(6)
$\text{S}(1)-\text{S}(3)$	3.368(9)	3.447(6)	$\text{S}(7)-\text{S}(10)$	3.309(9)	3.338(6)
$\text{S}(1)-\text{S}(5)$	3.237(9)	3.300(6)	$\text{S}(7)-\text{S}(11)$	3.394(9)	3.441(6)
$\text{S}(3)-\text{S}(5)$	3.463(9)	3.531(6)	$\text{S}(10)-\text{S}(11)$	3.439(9)	3.484(6)
$\text{S}(2)-\text{S}(4)$	3.540(9)	3.613(7)	$\text{S}(8)-\text{S}(9)$	3.257(9)	3.305(6)
$\text{S}(2)-\text{S}(6)$	3.279(9)	3.329(6)	$\text{S}(8)-\text{S}(12)$	3.523(9)	3.565(6)
$\text{S}(4)-\text{S}(6)$	3.426(9)	3.443(7)	$\text{S}(9)-\text{S}(12)$	3.403(9)	3.436(6)
$\text{S}(1)-\text{S}(6)$	3.416(9)	3.469(6)	$\text{S}(7)-\text{S}(9)$	3.354(9)	3.389(6)
$\text{S}(2)-\text{S}(3)$	3.570(10)	3.660(7)	$\text{S}(8)-\text{S}(11)$	3.539(10)	3.570(7)
$\text{S}(4)-\text{S}(5)$	3.540(9)	3.579(7)	$\text{S}(10)-\text{S}(12)$	3.417(9)	3.465(6)

Table 6. Selected interatomic distances (\AA) and angles ($^\circ$) in the six ligands.

Distances	150 K	295 K	Angles	150 K	295 K
Ligand 1					
S(1)–C(1)	1.656(22)	1.726(18)	S(1)–C(1)–S(2)	113.2(1.3)	111.4(1.0)
S(2)–C(1)	1.729(22)	1.723(18)	S(1)–C(1)–N(1)	124.8(1.7)	121.8(1.3)
C(1)–N(1)	1.319(28)	1.309(22)	S(2)–C(1)–N(1)	122.0(1.7)	126.5(1.4)
N(1)–C(2)	1.495(30)	1.421(20)	C(1)–N(1)–C(2)	119.8(1.8)	124.1(1.3)
N(1)–C(9)	1.485(30)	1.469(21)	C(1)–N(1)–C(9)	124.4(1.8)	120.4(1.4)
C(2)–C(3)	1.535(31)	1.512(21)	C(2)–N(1)–C(9)	115.7(1.7)	115.5(1.3)
C(9)–C(10)	1.503(31)	1.535(23)	N(1)–C(2)–C(3)	110.8(1.8)	114.1(1.3)
			N(1)–C(9)–C(10)	110.6(1.9)	110.3(1.3)
Ligand 2					
S(3)–C(16)	1.679(23)	1.703(17)	S(3)–C(16)–S(4)	109.9(1.2)	110.7(1.0)
S(4)–C(16)	1.773(24)	1.726(19)	S(3)–C(16)–N(2)	127.9(1.8)	125.2(1.4)
C(16)–N(2)	1.273(28)	1.315(21)	S(4)–C(16)–N(2)	121.4(1.7)	122.1(1.3)
N(2)–C(17)	1.441(29)	1.452(19)	C(16)–N(2)–C(17)	121.9(1.9)	121.1(1.3)
N(2)–C(24)	1.468(29)	1.459(21)	C(16)–N(2)–C(24)	126.5(1.9)	125.0(1.3)
C(17)–C(18)	1.516(28)	1.496(20)	C(17)–N(2)–C(24)	111.5(1.7)	113.9(1.2)
C(24)–C(25)	1.550(31)	1.499(23)	N(2)–C(17)–C(18)	112.1(1.8)	112.6(1.2)
			N(2)–C(24)–C(25)	115.4(1.8)	114.2(1.3)
Ligand 3					
S(5)–C(31)	1.655(25)	1.719(16)	S(5)–C(31)–S(6)	112.9(1.2)	112.8(0.9)
S(6)–C(31)	1.742(25)	1.692(16)	S(5)–C(31)–N(3)	128.3(1.8)	124.1(1.2)
C(31)–N(3)	1.391(27)	1.321(12)	S(6)–C(31)–N(3)	118.8(1.8)	122.9(1.2)
N(3)–C(32)	1.475(31)	1.460(20)	C(31)–N(3)–C(32)	123.5(1.9)	122.9(1.3)
N(3)–C(39)	1.425(29)	1.491(21)	C(31)–N(3)–C(39)	116.7(1.9)	118.7(1.2)
C(32)–C(33)	1.499(29)	1.461(21)	C(32)–N(3)–C(39)	118.3(1.7)	117.4(1.2)
C(39)–C(40)	1.549(40)	1.593(25)	N(3)–C(39)–C(40)	108.8(1.7)	109.6(1.3)
			N(3)–C(32)–C(33)	112.4(1.8)	113.0(1.3)
Ligand 4					
S(7)–C(46)	1.720(24)	1.707(17)	S(7)–C(46)–S(8)	112.6(1.4)	113.8(1.0)
S(8)–C(46)	1.688(24)	1.670(17)	S(7)–C(46)–N(4)	121.3(1.7)	121.4(1.2)
C(46)–N(4)	1.356(30)	1.363(21)	S(8)–C(46)–N(4)	126.0(1.8)	124.7(1.2)
N(4)–C(47)	1.504(29)	1.485(20)	C(46)–N(4)–C(47)	120.8(1.8)	122.8(1.2)
N(4)–C(54)	1.482(29)	1.501(19)	C(46)–N(4)–C(54)	120.4(1.8)	122.1(1.3)
C(47)–C(48)	1.490(30)	1.497(19)	C(47)–N(4)–C(54)	118.8(1.7)	115.1(1.2)
C(54)–C(55)	1.570(29)	1.509(20)	N(4)–C(54)–C(55)	106.4(1.4)	108.9(1.2)
			N(4)–C(47)–C(48)	112.3(1.8)	112.8(1.2)
Ligand 5					
S(9)–C(61)	1.711(23)	1.714(17)	S(9)–C(61)–S(10)	113.6(1.1)	111.0(0.8)
S(10)–C(61)	1.687(23)	1.734(17)	S(9)–C(61)–N(5)	123.0(1.6)	125.2(1.3)
C(61)–N(5)	1.365(24)	1.295(18)	S(10)–C(61)–N(5)	123.2(1.7)	123.7(1.3)
N(5)–C(62)	1.460(26)	1.489(19)	C(61)–N(5)–C(62)	125.0(1.7)	124.1(1.3)
N(5)–C(69)	1.505(28)	1.476(19)	C(61)–N(5)–C(69)	119.6(1.7)	121.2(1.3)
C(62)–C(63)	1.471(29)	1.463(21)	C(62)–N(5)–C(69)	115.4(1.4)	114.5(1.1)
C(69)–C(70)	1.533(30)	1.544(20)	N(5)–C(62)–C(63)	111.6(1.6)	111.6(1.2)
			N(5)–C(69)–C(70)	111.1(1.7)	111.0(1.2)

Table 6. Continued.

Ligand 6

S(11)–C(76)	1.755(22)	1.708(13)	S(11)–C(76)–S(12)	111.6(1.2)	112.5(0.7)
S(12)–C(76)	1.677(22)	1.716(11)	S(11)–C(76)–N(6)	120.7(1.6)	124.8(0.9)
C(76)–N(6)	1.302(28)	1.329(17)	S(12)–C(76)–N(6)	127.6(1.7)	122.7(1.0)
N(6)–C(77)	1.491(29)	1.473(20)	C(76)–N(6)–C(77)	119.3(1.8)	121.6(1.2)
N(6)–C(84)	1.539(29)	1.471(19)	C(76)–N(6)–C(84)	127.7(1.8)	122.2(1.2)
C(77)–C(78)	1.493(30)	1.492(20)	C(77)–N(6)–C(84)	112.8(1.6)	116.2(1.2)
C(84)–C(85)	1.541(30)	1.489(19)	N(6)–C(77)–C(78)	110.0(1.8)	110.7(1.2)
			N(6)–C(84)–C(85)	107.7(1.8)	119.9(1.2)

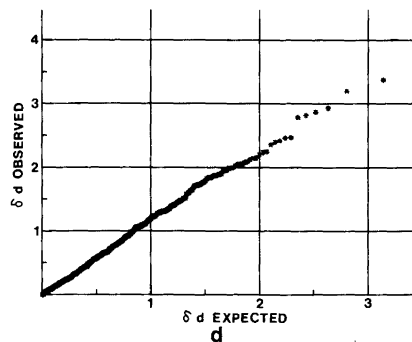
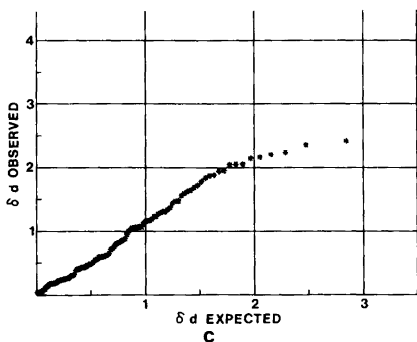
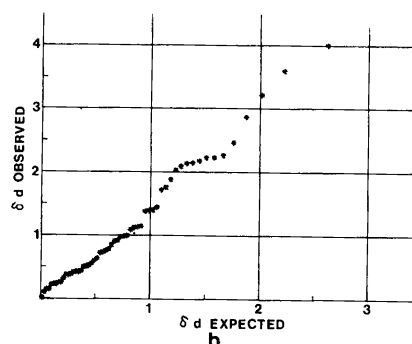
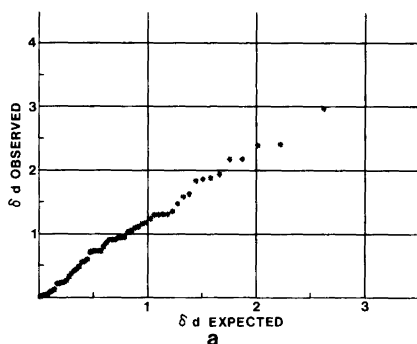


Fig. 6. Half-normal probability-plot comparison of interatomic distances in the ligands in $\text{Fe}[\text{S}_2\text{CN}(\text{CH}_2\text{C}_6\text{H}_5)_2]_3$; (a) 57 bond distances in Complex 1 and 2 at 150 K, slope: 1.18, intercept: 0.04; (b) d:o at 295 K, slope: 1.40, intercept: -0.01; (c) 114 bond distances at 150 and 295 K, slope: 1.17, intercept: -0.04; (d) all 296 bond distances $< 2.90 \text{ \AA}$, slope: 1.20, intercept: -0.03.

Table 7. Deviations ($\text{\AA} \times 10^3$) from the least-squares planes through the S_2CN groups. Atoms marked with an asterisk are not included in the LS-calculations.

150 K											
S(1)	0	S(3)	18	S(5)	4	S(7)	7	S(9)	-8	S(11)	5
S(2)	0	S(4)	16	S(6)	3	S(8)	7	S(10)	-8	S(12)	6
N(1)	-1	N(2)	26	N(3)	4	N(4)	10	N(5)	-11	N(6)	8
C(1)	1	C(16)	-59	C(31)	-11	C(46)	-23	C(61)	27	C(76)	-19
*C(2)	-33	*C(17)	118	*C(39)	315	*C(47)	111	*C(62)	33	*C(77)	138
*C(9)	-15	*C(24)	-58	*C(32)	19	*C(54)	-75	*C(69)	-168	*C(84)	-168
*Fe(1)	-383	*Fe(1)	-249	*Fe(1)	508	*Fe(2)	403	*Fe(2)	-283	*Fe(2)	470
295 K											
S(1)	-10	S(3)	1	S(5)	8	S(7)	-1	S(9)	-5	S(11)	1
S(2)	-11	S(4)	1	S(6)	8	S(8)	-1	S(10)	-5	S(12)	1
N(1)	-16	N(2)	2	N(3)	12	N(4)	-2	N(5)	-7	N(6)	2
C(1)	38	C(16)	-4	C(31)	-28	C(46)	4	C(61)	17	C(76)	-4
*C(2)	-100	*C(17)	111	*C(39)	303	*C(47)	53	*C(62)	14	*C(77)	158
*C(9)	-36	*C(24)	-81	*C(32)	37	*C(54)	-76	*C(69)	-154	*C(84)	-155
*Fe(1)	-431	*Fe(1)	-227	*Fe(1)	518	*Fe(2)	437	*Fe(2)	-299	*Fe(2)	433

these planes do not include the iron atoms. The geometries of the groups agree well with geometries found for corresponding groups in other dithiocarbamate compounds.^{4,11,15,16,24,25}

DISCUSSION

Besides the present compound we have also studied tris(1-pyrrolidinylcarbodithiato-S,S')iron(III) hemibenzene,¹⁶ tris(*N,N*-dimethylthiocarbamato)iron(III),⁴ and tris(*N,N*-di(2-hydroxyethyl)-dithiocarbamato)iron(III)¹⁵ at 150 and 295 K. Leipoldt and Coppens¹¹ have studied tris(*N,N*-diethyldithiocarbamato)iron(III) at 79 and 297 K. The solid 1-pyrrolidinyl substituted complex has been reported²⁶ as a high-spin compound with no sign of spin-state cross-over while the solid hemibenzene solvate of the same complex shows evidence of a decrease in μ_{eff} at very low temperatures. The curves of Fig. 2 indicate, however, that for both compounds there should be a substantial decrease in μ_{eff} with decreasing temperatures below 100 K. Sinn²⁶ has determined the structure at room temperature of the hemibenzene solvate. We have extended his measurements, so far to 150 K,¹⁶ but work at lower temperatures is in progress.

Table 8 gives the geometrical characteristics of the FeS_6 polyhedra. The octahedron is the ideal polyhedron with six vertices. In order to describe the distortions of the FeS_6 cores we have calculated the r.m.s. separation Δ after a best molecular fit of

the FeS_6 coordinates to those of the ideal octahedron.²⁷ A rotational fit routine without dilation was used²³ and the mean observed Fe–S distance was normalized to 1 Å. If ζ_i is the distance between vertex i in the octahedron and the corresponding vertex in the observed, fitted polyhedron we have

$$\Delta = \left[\sum_{i=1}^6 \zeta_i^2 / 6 \right]^{1/2}$$

The parameter Δ is a single measure of the distortion from ideal symmetry.

The geometry of the FeS_6 cores is governed by the Fe–S bond length. As can be seen in Table 8 the distortion is slightly worse at 295 than at 150 K. When the Fe–S bond distance decreases, the ligand bite (denoted a in Table 8) also decreases. On a scale related to the ligand bite the average edge length of the triangular faces then decreases while the relative height of the prism decreases or stays constant. This causes an increase in the torsion angle and thus a slightly better fit to the octahedron. (The torsion angle is calculated by method 1 of Ref. 28).

In a previous communication¹⁵ it was shown that there is an approximately curvilinear relationship between μ_{eff} and the mean observed Fe–S distance. For the six iron(III) dithiocarbamate complexes of Table 8 it is possible to compare the mean observed increase in Fe–S [denoted $\delta(\text{Fe–S})$] with the corresponding increase in μ_{eff} ($\Delta\mu_{\text{eff}}$). This is done in Fig. 7 and there is roughly a linear relationship

The geometry of the coordination polyhedra compared with the geometries of the O_6 and D_3 polyhedra. The quantities are explained in the text.

Complex	$\left[\text{Fe}[\text{S}_2\text{CN}(\text{CH}_2-\text{CH}_2)]_3 \right]_3$	$\left[\text{Fe}[\text{S}_2\text{CN}(\text{CH}_3)_2]_3 \right]_3$	$\left[\text{Fe}[\text{S}_2\text{CN}(\text{C}_2\text{H}_4\text{OH})_2]_3 \right]_3$	$\left[\text{Fe}[\text{S}_2\text{CN}(\text{CH}_2\text{C}_6\text{H}_5)_2]_3 \right]_3$	D_3
Γ (K)	150	295	150	295	150
t_{eff}	5.50	5.60	2.11	4.03	2.40
$\langle \text{Fe}-\text{S} \rangle (\text{\AA})$	2.427	2.435	2.339	2.395	2.331
$\Delta (\text{\AA})$	0.2887	0.2951	0.2759	0.2914	0.2817
Ligand bite ($S-S$) (\AA)	2.91	2.91	2.84	2.87	2.87
Edge of triangular face (\AA)	3.56 (1.22a)	3.57 (1.23a)	3.42 (1.20a)	3.52 (1.23a)	3.36 (1.18a)
Height of prism (\AA)	2.56 (0.88a)	2.59 (0.89a)	2.50 (0.88a)	2.53 (0.88a)	2.56 (0.90a)
Torsion angle ($^\circ$)	38	38	40	38	37
Tilt angle between the triangular faces ($^\circ$)	2.3	2.0	1.8	1.9	2.1
Fe(III)-centroid of the prisms (\AA)	0.08	0.05	0.03	0.04	0.01
	4	15	11	11	11
Reference	4	15	11	11	11

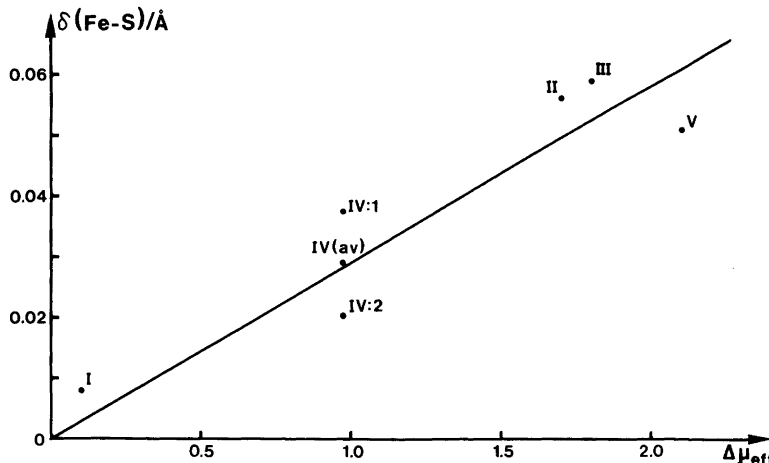


Fig. 7. The mean observed increase in Fe-S [$\delta(\text{Fe-S})$] as a function of the increase in the effective magnetic moment for five structures determined at low and room temperature; I: Tris(1-pyrrolidinylcarbodithiato-S,S')iron(III);¹⁶ II: Tris(*N,N*-dimethylthiocarbamato)iron(III);⁴ III: Tris[*N,N*-di(2-hydroxyethyl)dithiocarbamato]iron(III);¹⁵ IV: Tris(dibenzylidithiocarbamato)iron(III). Complex 1 and average value; V: Tris(*N,N*-diethyldithiocarbamato)iron(III).¹¹

between these quantities. A strict correlation is not to be expected since intermolecular forces will oppose changes in the coordination sphere in somewhat different ways in the five compounds. The values of the quantity $\delta(\text{Fe-S})$ is compatible with the difference, 0.10 Å, between the high and low-spin radii of Fe^{3+} .²⁹

The only significant changes detected in the complex geometries when μ_{eff} changes occur in the FeS_6 core. The ligands are unchanged except for the ligand bites. It could be argued that the increase in the metal-ligand π -bonding with decreasing μ_{eff} , i.e., decreasing temperature, which has been found in ^{13}C NMR experiments¹² gives rise to a decrease in the S-C and C-N bond lengths but that this decrease goes undetected because of the apparent lengthening of the bonds due to the decrease in thermal motion. That these two effects should cancel out in four structures is rather unlikely. If there is a change in the ligand geometry, it is on a scale below what can be detected with crystal structure determinations using X-ray diffraction methods.

Acknowledgements. We thank Dr. Mats Nygren for measuring the data presented in Fig. 2. The Swedish Natural Science Council gave financial support.

REFERENCES

- White, A. H., Roper, R., Kokot, E., Waterman, H. and Martin, R. L. *Aust. J. Chem.* 17 (1964) 294.
- Ewald, A. H., Martin, R. L., Ross, I. G. and White, A. H. *Proc. R. Soc. London A* 280 (1964) 235.
- Ewald, A. H., Martin, R. L., Sinn, E. and White, A. H. *Inorg. Chem.* 8 (1969) 1837.
- Albertsson, J. and Oskarsson, Å. *Acta Crystallogr. B* 33 (1977) 1871.
- Herrithew, P. B. and Rasmussen, P. G. *Inorg. Chem.* 11 (1972) 325.
- Butcher, R. J. and Sinn, E. *J. Am. Chem. Soc.* 98 (1976) 2440, 5159.
- Butsher, R. J., Ferraro, J. R. and Sinn, E. *Inorg. Chem.* 15 (1976) 2077.
- Flick, C. and Gelerinter, E. *Chem. Phys. Lett.* 23 (1973) 422.
- Sorai, M. *J. Inorg. Nucl. Chem.* 40 (1978) 1031.
- Eley, R. R., Duffy, N. V. and Uhrich, D. L. *J. Inorg. Nucl. Chem.* 34 (1972) 3681.
- Leipoldt, J. G. and Coppens, P. *Inorg. Chem.* 12 (1973) 2269.
- Gregson, K. and Doddrell, D. M. *Chem. Phys. Lett.* 31 (1975) 125.
- Cukauskas, E. J. *Magnetic Susceptibility Measurements Using Supraconducting Devices*, Thesis, University of Virginia, Virginia 1974.

14. Cukauskas, E. J., Deaver, B. S. and Sinn, E. *J. Chem. Phys.* 67 (1977) 1257.
15. Albertsson, J., Nygren, M. and Oskarsson, Å. *Acta Crystallogr. B* 39. *In press.*
16. Albertsson, J. and Oskarsson, Å. *To be published.*
17. Nygren, M. *Private communication.*
18. Blom, B. and Hörlin, T. *Chem. Commun. Univ. Stockholm* (1977) No. 5.
19. Buerger, M. J. *Vector Space*, Wiley, New York 1959.
20. Danielsson, S., Grenthe, I. and Oskarsson, Å. *J. Appl. Crystallogr.* 9 (1976) 14.
21. *International Tables for X-Ray Crystallography*, Kynoch Press, Birmingham 1974, Vol. IV.
22. Abrahams, S. C. and Keve, E. T. *Acta Crystallogr. A* 27 (1971) 157.
23. Albertsson, J. and Svensson, C. *To be published.*
24. Jennische, P. and Hesse, R. *Acta Chem. Scand.* 27 (1973) 3531.
25. Einstein, F. W. B. and Field, J. S. *Acta Crystallogr. B* 30 (1974) 2928.
26. Sinn, E. *Inorg. Chem.* 15 (1976) 369.
27. Dollase, W. A. *Acta Crystallogr. A* 30 (1974) 518.
28. Dymock, K. R. and Palenik, G. J. *Inorg. Chem.* 14 (1975) 1220.
29. Shannon, R. D. *Acta Crystallogr. A* 32 (1976) 751.

Received May 16, 1979.